Inorganic Chemistry

Article

pubs.acs.org/IC

Ligand Dynamics of *tert*-Butyl Isocyanide Oxido Complexes of Molybdenum(IV)

Jana Leppin, Christoph Förster, and Katja Heinze*

Institute of Inorganic Chemistry and Analytical Chemistry, Johannes Gutenberg-University of Mainz, Duesbergweg 10−14, 55128 Mainz, Germany

Supporting Information

ABSTRACT: The six-coordinate molybdenum(IV) oxido isocyanide complex **1** [Δ,Λ-OC-6-2-3-[MoO(N^p∩N^i)$_2$(CN^tBu)]; N^p∩N^i = 4-*tert*-butylphenyl(pyrrolato-2-ylmethylene)amine] is obtained in diastereomerically pure form in the solid state, as revealed by single-crystal X-ray diffraction. In solution, this stereoisomer equilibrates with the Δ,Λ-OC-6-2-4 diastereomer **2** at ambient temperature. The stereochemistry of both isomers has been elucidated by NMR, IR, and UV/vis spectroscopy in combination with density functional theory (DFT)/polarizable continuum model and time-dependent DFT calculations. The isomerization **1** → **2** is suggested to proceed via a dissociative trigonal twist with dissociation of the imine nitrogen donor N^i of one chelate ligand (hemilabile ligand) rather than dissociation of the monodentate isocyanide ligand. The isomerization barrier has been experimentally determined as 91 and 95 kJ mol^{-1} in tetrahydrofuran and toluene, respectively.

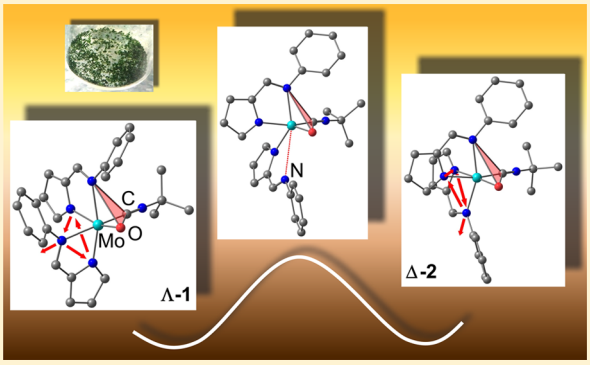

INTRODUCTION

Oxidomolybdenum complexes are known to catalyze oxygen-atom-transfer (OAT) reactions between closed-shell molecules.[1] A tremendous amount of work has been devoted to elucidate the mechanism with respect to biomimetic and other useful OAT reactions. Especially, molybdenum oxotransferase model systems have been studied in considerable detail.[2] Molybdenum-dependent carbon monoxide dehydrogenases (CODHs) catalyze the reaction CO + H_2O → CO_2 + 2e$^-$ + 2H$^+$. The enzyme contains a unique molybdopterin−molybdenum active site in combination with a copper center connected by a sulfido bridge (Scheme 1).[3] In the *n*-butylisocyanide-inhibited form of CODH, a bridging thiocarbamate is formed with N-coordinated copper (Scheme 1).[3] A seminal structural model for molybdenum-dependent CODH with a Mo^VO−μ-S−Cu^I core has been reported by Young et al.[4] Hofmann et al. suggested that CO_2 elimination occurs from molybdenum-bound κ^2-(*O*,*C*)-CO_2 (Scheme 1), while according to Siegbahn and Shestakov, CO_2 is released from the copper center (Scheme 1).[5,6] In any case, the catalytic cycle is completed by double deprotonation and double oxidation of the molybdenum(IV) intermediate.

Molecular precedence for Mo═O nucleophilic attack at [L_nMCO]$^+$, giving μ$_2$-η^3-CO_2 ligands, has been reported by employing electron-rich 18 valence-electron $Mo^{IV}Cp_2$(═O) complexes and cationic carbonyl complexes.[7] Recently, a rather electrophilic Mo^{IV}Cp*(amidato)(≡O) complex was found to oxygenate CN^tBu to OCN^tBu via a Mo^{II}Cp*(amidato)(κ^2-(*O*,*C*)-OCN^tBu)(CN^tBu) intermediate in the presence of excess CN^tBu.[8] However, Mo^{II} oxidation states have been neither observed nor postulated in molybdenum-containing oxygenases.

Thus, we aimed at preparing analogue systems that bind a carbon-based substrate at molybdenum in biologically relevant

Scheme 1. (Top) Suggested Intermediates by Hofmann et al.[5] and Siegbahn and Shestakov[6] (S∩S = molybdopterin; X = O, NR) of Molybdenum-Dependent CODH and (Bottom) OAT between Molybdenum(IV) Oxido and Molybdenum(IV) Complexes with the Chelate Ligand N^p∩N^i

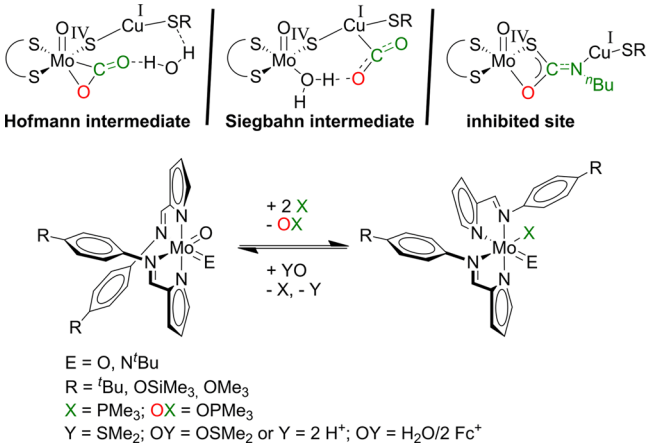

Received: October 4, 2013
Published: January 6, 2014

   dx.doi.org/10.1021/ic4025102 | *Inorg. Chem.* 2014, 53, 1039−1047

oxidation states below VI+, i.e., V+ and IV+. Recently, we had described a molybdenum(VI,V,IV) system with unsymmetrical Schiff base ligands 4-*tert*-butylphenyl(pyrrolato-2-ylmethylene)-amine ($N^p \cap N^i$, where N^i = imine nitrogen atom and N^p = pyrrolato nitrogen atom; Scheme 1) capable of catalytically transferring oxygen atoms to phosphanes as substrates from dimethyl sulfoxide or from a water/ferrocenium oxidant as terminal oxygen donors.[9−11] As a quite stable and fully characterized intermediate in the catalytic cycle, we isolated the $Mo^{IV}O(N^p \cap N^i)_2(PMe_3)$ complex with a further substrate, stabilizing the Mo^{IV} core. Similarly, the analogous imido complex $Mo^{IV}(N^tBu)(N^p \cap N^i)_2(PMe_3)$ and its one-electron-oxidized redox congener $[Mo^{V}(N^tBu)(N^p \cap N^i)_2(PMe_3)]^+$ have been isolated and fully characterized by NMR and electron paramagnetic resonance spectroscopy, density functional theory (DFT) calculations, and X-ray diffraction (Scheme 1).[12] We thus speculated that *tert*-butyl isocyanide as a CO surrogate could be coordinated to Mo^{IV} (and possibly also to Mo^{V}) in place of PMe_3 in a similar ligand environment, leading to precedence of truncated (copper-deficient) potential intermediates $MoO(N^p \cap N^i)_2(CN^tBu)$ or $Mo(N^p \cap N^i)_2(OCN^tBu)$. With this background, we investigated the preparation, isolation, and stability/lability of molybdenum oxido isocyanide complexes based on the chelate ligand system $N^p \cap N^i$.

Typical experimental access pathways to $Mo^{IV}O(CN^tBu)$ complexes involve CN^tBu substitution in *trans*-$Mo^{IV}(Cl)O(CN^tBu)_4$[13,14] by chelating ligands,[15,16] N_2 substitution in $Mo^{III}(N_2)$ complexes by CN^tBu and subsequent oxidation to Mo^{IV}[17] and ligand exchange at molybdenum(IV) phosphane complexes.[18,19] Oxidative addition of OCN^tBu has been reported to be viable for tungsten(II) complexes possibly via a κ^2-(*O*,*C*)-OCN^tBu intermediate,[20] while oxidative addition of OCN^tBu to Mo^{II} only yields a $Mo^{IV}(N^tBu)(CO)$ complex.[21]

EXPERIMENTAL SECTION

General Procedures. All reactions were performed under an inert atmosphere (Schlenk techniques, glovebox). Tetrahydrofuran (THF) was distilled from potassium, diethyl ether, and petroleum ether (bp 40−60 °C) and triethylamine from calcium hydride. The Schiff base ligand $HN^p \cap N^i$ and the phosphane complex $Mo^{IV}O(N^p \cap N^i)_2(PMe_3)$ were prepared according to literature procedures.[12] All other reagents were used as received from commercial suppliers (Acros, Sigma-Aldrich). NMR spectra were recorded on a Bruker Avance DRX 400 spectrometer at 400.31 MHz (^{1}H), 100.66 MHz (^{13}C{^{1}H}), and 40.56 MHz (^{15}N). All resonances are reported in ppm versus the solvent signal as the internal standard [THF-d_8 (^{1}H, δ 1.73, 3.58; ^{13}C, δ 25.37, 67.57)] versus external CH_3NO_2 [90% in $CDCl_3$ (^{15}N, δ 380.23)]. ^{15}N data are reported versus liquid NH_3 as the reference (δ 0). IR spectra were recorded with a BioRad Excalibur FTS 3100 spectrometer as CsI disks or in KBr cells in solution. UV/vis/near-IR spectra were recorded on a Varian Cary 5000 spectrometer using 1.0 cm cells (Hellma, Suprasil). Field-desorption (FD) mass spectra were recorded on a FD Finnigan MAT95 spectrometer. Elemental analyses were performed by the microanalytical laboratory of the Chemical Institutes of the University of Mainz.

Crystal Structure Determination. Intensity data were collected with a Bruker AXS Smart 1000 CCD diffractometer with an APEX II detector and an Oxford cooling system and corrected for absorption and other effects using Mo Kα radiation (λ = 0.71073 Å) at 173(2) K. The diffraction frames were integrated using the *SAINT* package, and most were corrected for absorption with *SADABS*.[22,23] The structure was solved by direct methods and refined by the full-matrix method based on F^2 using the *SHELXTL* software package.[24,25] All non-hydrogen atoms were refined anisotropically, while the positions of all hydrogen atoms were generated with appropriate geometric constraints and allowed to ride on their respective parent carbon atoms with fixed isotropic thermal parameters. The THF solvate molecule shows pseudorotational disorder with occupancy factors of 0.3 and 0.7. Crystallographic data (excluding structure factors) for the structure reported in this paper have been deposited with the Cambridge Crystallographic Data Centre as supplementary publication CCDC 952600. Copies of the data can be obtained free of charge upon application to CCDC, 12 Union Road, Cambridge CB2 1EZ, U.K. [fax (0.44) 1223-336-033; e-mail deposit@ccdc.cam.ac.uk].

Crystallographic data of 1: $C_{39}H_{51}MoN_5O_2$ (717.79); orthorhombic; *Pbca*; a = 17.7739(13) Å, b = 16.1821(9) Å, c = 25.8978(16) Å, V = 7448.7(8) Å^3; Z = 8; density, calcd = 1.280 g cm^{-3}, μ = 0.391 mm^{-1}; F(000) = 3024; crystal size 0.50 × 0.35 × 0.20 mm; θ = 1.57−28.02°; $-23 \le h \le 23$, $-21 \le k \le 17$, $-34 \le l \le 34$; reflns collected = 49312; reflns unique = 8995 [R(int) = 0.0479]; completeness to θ = 28.02° = 99.7%; semiempirical absorption correction from equivalents; max and min transmission = 0.926 and 0.828; no. of data = 8995; no. of restraints = 0; no. of parameters = 442; GOF on F^2 = 1.138; final R indices [$I > 2\sigma(I)$] of R1 = 0.0323, wR2 = 0.0763; R indices (all data) of R1 = 0.0552, wR2 = 0.0909; largest difference peak and hole = 0.339 and −0.357 e Å^{-3}.

DFT calculations were carried out with the *Gaussian09/DFT*[26] series of programs. The B3LYP formulation of DFT was used by employing the LANL2DZ basis set supplemented by d-type polarization functions[27] on nitrogen (ζ = 0.864) and oxygen (ζ = 1.154). All structures were characterized as minima or first-order saddle points by frequency analysis (N_{imag} = 0, 1). No symmetry constraints were imposed on the molecules. Solvent modeling was done by employing the integral equation formalism polarizable continuum model (IEFPCM, THF). The modeled complexes were slightly simplified by replacing the *tert*-butyl group of the chelate ligands by hydrogen atoms. The approximate free energies at 298 K were obtained through thermochemical analysis of the frequency calculation, using the thermal correction to the Gibbs free energy, as reported by *Gaussian09*.

Synthesis of 1/2. $Mo^{IV}O(N^p \cap N^i)_2(PMe_3)$[12] (350 mg, 0.55 mmol) was dissolved in THF (6 mL), and *tert*-butyl isocyanide (620 μL, 5.5 mmol) was added. The mixture was stirred for 24 h at 50 °C under a slow flow of argon, removing the volatile PMe_3. After cooling to room temperature, all volatiles were removed under reduced pressure to give the **1**/**2** mixture as a green powder in essentially quantitative yield.

Isolation of 1 from the 1/2 Mixture. By recrystallization of the **1**/**2** mixture from petroleum ether (bp 40−60 °C) at 8 °C, isomerically pure crystalline **1** was isolated in 21% yield (74 mg, 0.12 mmol). Elem anal. Calcd for $C_{35}H_{43}N_5OMo$ (645.70)·$^1/_2$hexane: C, 66.26; H, 7.32; N, 10.17. Found: C, 66.87; H, 7.54; N, 10.67. FD-MS: m/z (%) = 647.4 (22) ([M]$^+$; correct isotopic distribution), 564.4 (9) ([M − CNtBu]$^+$). IR (CsI): $\tilde{\nu}$ 3092 (w, CH_{ar}), 2962 (m, CH_{al}), 2129 (m, C≡N), 1568 (vs), 1508 (m), 1392 (m), 1291 (s), 1179 (m), 1036 (s), 937 (vs, Mo═O), 756 (vs), 746 (vs) cm^{-1}. UV/vis [THF; λ_{max}, nm (ε, M^{-1} cm^{-1})]: 255 (22605, sh), 307 (31265), 402 (12355), 540 (2440). ^{1}H NMR (THF-d_8): δ 8.13 (s, 1H, H^{7b}), 7.69 (s, 1H, H^{11b}), 7.44 (s, 1H, H^{7a}), 7.24 (d, $^3J_{HH}$ = 8.7 Hz, 2H, H^{3a,5a}), 7.15 (d, $^3J_{HH}$ = 8.7 Hz, 2H, H^{3b,5b}), 7.06 (d, $^3J_{HH}$ = 8.7 Hz, 2H, H^{2a,6a}), 7.01 (dvd, 1H, H^{9b}), 6.77 (d, $^3J_{HH}$ = 8.7 Hz, 2H, H^{2b,6b}), 6.47 (dvd, 1H, H^{10b}), 6.28 (dvd, 1H, H^{9a} or H^{10a}), 5.75 (m, 1H, H^{11a}), 5.73 (dvd, 1H, H^{9a} or H^{10a}), 1.44 (s, 9H, H^{16a,b}), 1.35 (2 s, 18H, H^{13a,b}). ^{13}C{^{1}H} NMR (THF-d_8): δ 158.9 (s, C^{7b}), 153.0 (s, C^{7a}), 152.4 (s, C^{1a}), 150.5 (s, C^{1b}), 148.7 (s, C^{4a}), 149.2 (s, C^{4b}), 146.9 (s, C^{11b}), 144.4 (s, C^{8b}), 140.9 (s, C^{8a}), 137.9 (s, C^{11a}), 126.3 (s, C$^{3b/5b}$), 125.7 (s, C$^{3a/5a}$), 124.3 (s, C$^{2a/6a}$), 123.1 (s, C$^{2b/6b}$), 119.6 (s, C^{9b}), 116.1 (s, C^{9a} or C^{10a}), 115.1 (s, C^{10b}), 113.6 (s, C^{9a} or C^{10a}), 60.6 (s, C≡NC(CH$_3$)$_3$), 35.0 (s, C^{12a,12b}), 31.9 (s, C^{13a,13b}), 31.0 (s, C≡NC(CH$_3$)$_3$); the resonance of C≡NC(CH$_3$)$_3$ is not observed. ^{15}N NMR (THF-d_8): δ 274.9 (N≡C), 238.2 (N^{i,b}), 232.7 (N^{p,a}), 230.2 (N^{i,a}), 220.2 (N^{p,b}).

Synthesis of the 1/2 Isomer Mixture. A THF solution of **1** was allowed to equilibrate at room temperature for at least 2 h, and the spectroscopic data for **2** were determined from this equilibrium mixture. ^{1}H NMR (THF-d_8): δ 8.41 (s, 1H, H^{7d}), 7.99 (s, 1H, H^{7c}), 7.74 (d, $^3J_{HH}$ = 8.7 Hz, 2H, H^{2c,6c}), 7.60 (d, $^3J_{HH}$ = 8.7 Hz, 2H, H^{2d,6d}), 7.52 (d, $^3J_{HH}$ = 8.7 Hz, 2H, H^{3d,5d}), 7.44 (d, $^3J_{HH}$ = 8.7 Hz, 2H, H^{3c,5c}),

dx.doi.org/10.1021/ic4025102 | *Inorg. Chem.* 2014, 53, 1039−1047

7.34 (m, 1H, H^{11d}), 6.98 (dvd, 1H, H^{9d}), 6.42 (m, 1H, H^{11c}), 6.35 (dvd, 1H, H^{9c}), 6.21 (dvd, 1H, H^{10d}), 5.78 (dvd, 1H, H^{10c}), 1.38 (2 s, 18H, $H^{13c,13d}$) 1.01 (s, 9H, $H^{16c,16d}$). $^{13}C\{^1H\}$ NMR (THF-d_8): δ 157.8 (s, C^{7d}), 151.4 (s, C^{7c}), 154.1 (s, C^{1d}), 151.1 (s, C^{1c}), 149.2 (2 s, $C^{4c,4d}$), 143.3 (s, C^{8d}), 141.4 (s, C^{8c}), 141.5 (s, C^{11d}), 138.1 (s, C^{11c}), 126.6 (s, $C^{3d/5d}$), 126.5 (s, $C^{3c/5c}$), 123.4 (s, $C^{2c/6c}$), 123.3 (s, $C^{2d/6d}$), 121.6 (s, C^{9d}), 117.5 (s, C^{9c}), 115.0 (s, C^{10d}), 113.6 (s, C^{10c}), 58.7 (s, $C{\equiv}NC(CH_3)_3$), 35.2 (s, $C^{12c,12d}$), 31.9 (s, $C^{13c,13d}$), 30.2 (s, $C{\equiv}NC(CH_3)_3$); the resonance of $C{\equiv}NC(CH_3)_3$ is not observed. ^{15}N NMR (THF-d_8): δ 250.5 (N≡C), 231.5 ($N^{p,d}$), 228.6 ($N^{p,c}$), 225.2 ($N^{i,c}$), 221.3 ($N^{i,d}$). UV/vis [λ_{max}, nm (ε, M^{-1} cm^{-1})]: 235 (19765), 307 (35700), 449 (9970), 537 (7705) (data obtained from the difference spectrum "**1**/**2** mixture *minus* **1**").

Reaction of A with Excess CN^{t}Bu. The dioxido complex **A** (20 mg, 0.034 mmol) was dissolved in toluene (4 mL), and CN^{t}Bu (14.3 mg, 0.17 mmol) was added. The solution was heated to 95 °C for several hours, and ^{1}H NMR spectra were measured. After 5.5 h, the only resonances observed are those of **A**, CN^{t}Bu, and free chelate ligand.

Reaction of 1/2 with Water/Base. The isomer mixture **1**/**2** (13.2 mg, 0.02 mmol) was dissolved in THF-d_8 (1 mL). Phosphazene base *tert*-butyliminotris(dimethylamino)phosphorane ($P_1{}^t$Bu; 9.56 mg, 0.04 mmol) and water (0.74 μL, 0.04 mmol) were added. According to ^{1}H NMR spectra, the mixture remained unchanged for several weeks in solution at room temperature, except for some chelate ligand dissociation.

RESULTS AND DISCUSSION

Synthesis. The previously reported molybdenum(VI) complex $Mo^{VI}O_2(N^p{\cap}N^i)_2$ (**A**) is competent to oxygenate phosphanes, e.g., PMe_3, giving the molybdenum(IV) phosphane complex $Mo^{IV}O(N^p{\cap}N^i)_2(PMe_3)$ (**B**) and phosphane oxide.[9−12] In an analogous experiment, **A** is treated with excess *tert*-butyl isocyanide, but OAT to CN^{t}Bu is not observed either at room temperature or at elevated temperature (95 °C, toluene).

Coordination of CN^{t}Bu at the molybdenum(IV) center to give $Mo^{IV}O(N^p{\cap}N^i)_2(CN^tBu)$ was achieved by PMe_3 substitution[18,19] from molybdenum(IV) complex **B** and permanently removing the liberated volatile PMe_3 by a slow flow of argon to drive the reaction to completion (Scheme 2). According to IR and NMR spectroscopy (vide infra), no attack at the oxido ligand of the $Mo^{IV}O$ unit to give coordinated (or liberated) OCN^{t}Bu and Mo^{II} was observed, as has been demonstrated for a $Mo^{IV}Cp^*$(amidato)(O) complex and CN^{t}Bu, giving a κ^2-(*C*,*O*)-OCN^{t}Bu-coordinated molybdenum(II) complex.[8]

Scheme 2. Synthesis of Molybdenum(IV) Oxido *tert*-Butyl Isocyanide Complexes from the Dioxido Complex A via the Phosphane Complex B

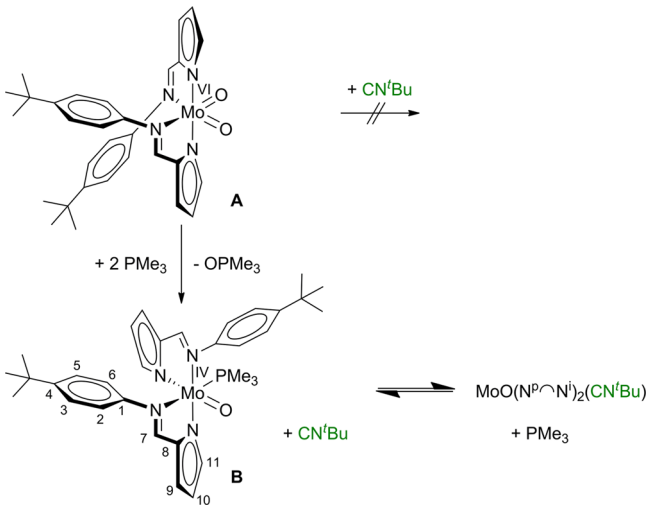

Stereochemistry. After recrystallization of the resulting green material with the composition $Mo^{IV}O(N^p{\cap}N^i)_2(CN^tBu)$ (by mass spectrometry) from 1:2 THF/petroleum ether (bp 40−60 °C), the ^{1}H NMR spectrum of the green compound, taken immediately after dissolution, features resonances corresponding to two chelate ligands $N^p{\cap}N^i$ and one coordinated isocyanide ligand (δ 1.44) in the expected intensity ratio (Figure 1, bottom). Upon standing at room temperature, these resonances lose intensity. Concomitantly, new resonances corresponding to two further chelate ligands (14 ^{1}H resonances) and one isocyanide ligand (δ 1.01) develop (Figure 1). A stationary state is reached after approximately 2 h (≈2:1 ratio). At higher temperature, the equilibrium composition does not change appreciably, suggesting only small entropy changes during the reaction. Resonances corresponding to four chelate ligands $N^p{\cap}N^i$ and two isocyanides in total are also detected in the $^{13}C\{^1H\}$ NMR and the $^1H{,}^{15}N$ HMBC spectra (4 × N^p, 4 × N^i, and 2 × $N^{isocyanide}$; Figures S1 and S2 in the SI). These observations clearly point to an equilibrium between two stereoisomers in solution (Scheme 2 and Chart 1). As can be seen from Figure 1, tiny amounts of other diastereomers are also formed.

In order to assign the configuration of the isomers formed, nuclear Overhauser effect (NOE) spectral data were acquired and analyzed with the aid of DFT models (Figure 2 and Table 1; B3LYP/LANL2DZ/PCM). Short distances between the isocyanide protons and the chelate ligand orthogonal to the Mo−C vector (ligands a, c, e, and g in **1**−**4**) are possible in all stereoisomers and are thus inconclusive for assignments of the stereochemistry (Figure 2). However, short distances between the isocyanide protons and the second chelate (ligands b, d, f, and h in **1**−**4**) discriminate between pairs of stereoisomers **1**/**3** and **2**/**4**. Stereoisomers **1** and **3** show a short contact to H^{11} (pyrrolate of ligands b and f coplanar to isocyanide Mo−CN; $d \leq 3$ Å), while diasteromers **2** and **4** feature short contacts to $H^{2/6}$ and $H^{3/5}$ (N^iAr of ligands d and h coplanar to isocyanide Mo−CN; $d \leq 2.2$ Å). The major isomer present at the beginning of the isomerization directly after dissolution displays five NOE cross peaks between the isocyanide protons (δ 1.44) and one chelate ligand, as expected, and a further cross peak to H^{11} of the second chelate, which is hence compatible with configurations **1** and **3**, respectively (Figure 2 and Chart 1). The second (minor) isomer progressively formed at $T > -30$ °C gives three NOE cross peaks between the isocyanide protons (δ 1.01) and the chelate ligands. Contacts are established between the isocyanide and the pyrrole proton H^{11} of one chelate and the aromatic protons $H^{2,6}$ and $H^{3,5}$ of the other chelate. These contacts are compatible with configurations **2** and **4** (Chart 1).

Fortunately, single crystals of the isocyanide complex were obtained from a 1:2 THF/petroleum ether (bp 40−60 °C) solution at 8 °C. X-ray diffraction analysis (orthorhombic *Pbca*, THF solvate) substantiates configuration **1** (OC-6-2-3) in the crystalline state (Figure 3). The experimental metrical data of the complex also fit to the DFT-calculated data of stereoisomer **1** (Table 1). The Mo═O distance of 1.685 Å is similar to that of the PMe_3 complex **B** [$Mo^{IV}O(N^p{\cap}N^i)_2(PMe_3)$ with analogous stereochemistry: d(Mo−O) = 1.686 Å][12] and to that of a molybdenum(IV) oxido bis(isocyanide) complex with

dx.doi.org/10.1021/ic4025102 | *Inorg. Chem.* 2014, 53, 1039−1047

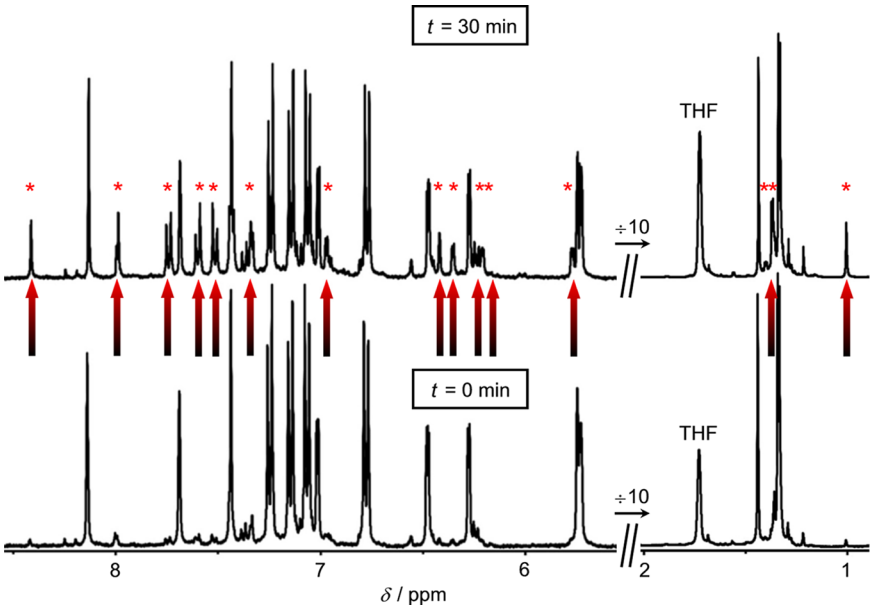

Figure 1. ^{1}H NMR spectra of $Mo^{IV}O(N^p \cap N^i)_2(CN^tBu)$ in THF-d_8 directly after dissolution of crystals (bottom) and after 30 min (top) at 25 °C. Growing resonances are marked with asterisks and arrows.

Chart 1. Possible Diastereomers 1−4, Stereodescriptors Based on the CIP Priorities[28−32] Shown in Red, and Indicated Chelate Ligands a−h (Corresponding Δ Enantiomers Not Shown)

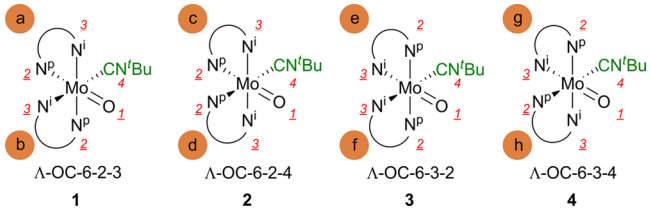

a tris(mercaptoimidazolyl)borate ligand [d(Mo−O) = 1.684 Å].[15] The Mo−C bond lengths of the latter complex are smaller [d(Mo−C) = 2.021/2.075 Å] than that of **1** [d(Mo−C) = 2.109 Å]. No O···C interaction is observed in **1** [d(O···C) = 2.785 Å], as found in the complex MoCp*(amidato)(κ^2-(O,C)-OCN^{t}Bu)(CN^{t}Bu) [d(O···C) = 1.307 Å] with side-on κ^2-(O,C)-OCN^{t}Bu coordination.[8]

Having assigned the OC-6-2-3 configuration to isomer **1** present in the solid state, we attempted to elucidate the configuration of the second isomer (**2** or **4** according to NOE data). Solid-state IR spectra recorded for the recrystallized material (pure isomer **1**) feature an absorption band for the CN stretching mode at $\tilde{\nu}_{CN}$ = 2129 cm^{-1}, while the precipitated raw material of the isomer mixture shows a broad absorption band at $\tilde{\nu}_{CN}$ = 2142 cm^{-1} (Figure S3 in the SI). DFT calculations and harmonic frequency calculations yield CN stretching vibrations for the stereoisomers **1**−**4** at $\tilde{\nu}_{CN}$ = 2117, 2124, 2113, and 2113 cm^{-1}, respectively (Table 1, scaled by 0.9614[33]). These data support configuration **1** for the major isomer and suggest configuration **2** for the minor isomer with a slightly higher CN stretching frequency than **1**. Because both configurations **3** and **4** possess lower CN stretching frequencies than **1** according to the calculations, they are likely excluded as minor isomers.

In addition, the Mo═O stretching vibrations are calculated with very similar energies for the pairs **1**/**2** (anionic pyrrolate trans to oxido; 947/946 cm^{-1}) and **3**/**4** (π-accepting imine trans to oxido; 965/967 cm^{-1}). The recrystallized material displays $\tilde{\nu}_{MoO}$ = 937 cm^{-1}, similar to the raw material ($\tilde{\nu}_{MoO}$ = 939 cm^{-1}; Figure S3 in the SI). Because the Mo═O stretching mode is essentially insensitive to the nature of the cis ligands but very sensitive to the trans ligand,[14] the $\tilde{\nu}_{MoO}$ data suggest that the trans ligand remains at its position during isomerization. Thus, according to the Mo═O stretching mode, **1** is transformed to **2** or **3** to **4**, with the latter case being excluded on the basis of the CN stretch and X-ray diffraction. Thus, all available data point to the isomerization of **1** to **2** being operative with only minor isomerization to isomers **3** or **4**. Gratifyingly, the two isomers **1** and **2** are also calculated as the most stable ones by DFT calculations (Table 1). In a THF solution, the CN stretching vibration shifts from $\tilde{\nu}_{CN}$ = 2135 cm^{-1} (**1**) to 2138 cm^{-1} (mixture of **1** and **2**) within 2 h at room temperature.

Similar to evolution of the NMR and IR spectra, the optical properties change upon dissolution of crystals of **1** in THF until equilibrium is reached (Figure 4). From the NMR data, the final ratio (≈2:1 at 298 K) is known. With this ratio, the approximate spectrum of the minor isomer can be extracted from the final UV/vis spectrum (Figure 5, top; note that other isomers formed in tiny amounts are neglected). The π−π* absorptions of the minor isomer are more intense than those found for **1** (≈1:1.14) but remain essentially unshifted (λ_{max} = 307 nm), and an absorption window (≈390−400 nm) arises between the π−π* and ligand field/CT bands in the minor isomer.

In order to identify significant optical differences among isomers **1**−**4**, TD-DFT calculations have been performed (Figure 5, bottom). Isomers **1** and **2** feature π−π* absorptions calculated at similar energy [λ_{max}(**1**) = λ_{max}(**2**) = 307 nm] with a higher intensity for **2** (**1**:**2** ≈ 1:1.35). On the other hand, isomers **3** and **4** are calculated to possess bathochromically shifted π−π* bands [λ_{max}(**3**) = 332 nm and λ_{max}(**4**) = 326 nm] with lower intensity compared to **1** (**1**:**3** ≈ 1:0.86 and **1**:**4** ≈ 1:0.87). The data pertaining to **3** and **4** are thus incompatible with the experimental findings (Figure 5). Furthermore, isomer **1** features a CT absorption band at 402 nm (Figure 5, top),

dx.doi.org/10.1021/ic4025102 | Inorg. Chem. 2014, 53, 1039−1047

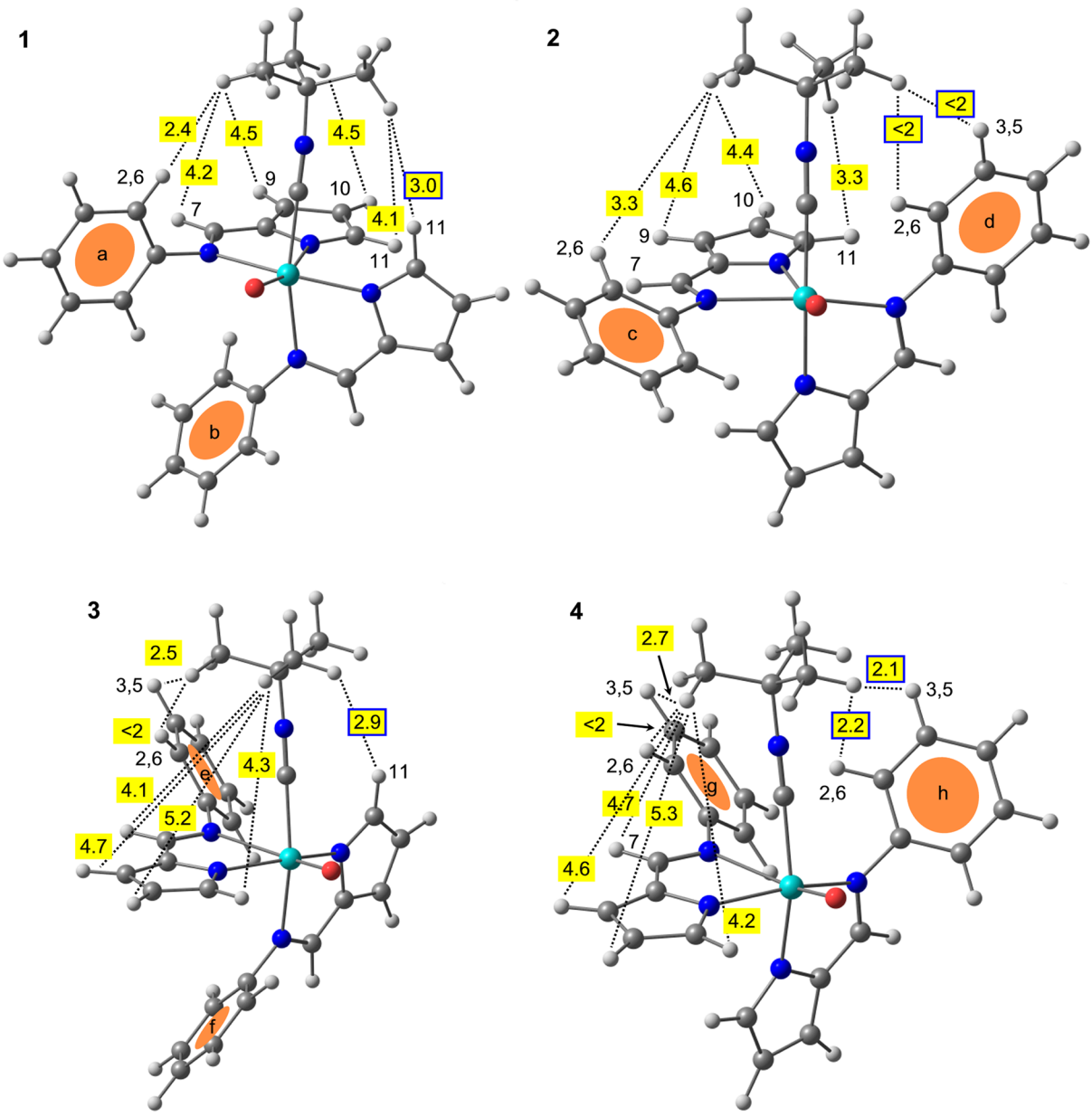

Figure 2. DFT-calculated minimum geometries of stereoisomers **1**−**4** and relevant interligand H···H distances (minimum distances/Å achievable by rotation and torsion around single bonds).

which is calculated around 355 nm by TD-DFT (Figure 5, bottom). The transitions of this band at 347/364 nm (f = 0.055/0.050) are basically pyrrolate to π^*(MoO/imine) in character. For isomer **2**, the energies of these transitions are more distinct and the intensities are much weaker (354/380 nm, f = 0.014/0.014), resulting in less absorption in the spectral region of the CT transitions, in agreement with the experiment (Figure 5). On the basis of the combined NMR, IR, and UV/vis data, we assign configuration **2** (OC-6-2-4) to the minor isomer with high confidence.

Kinetics of Isomerization. In general, the isomerization of **1** to **2** (and to other diastereomers and enantiomers) could proceed via a trigonal-twist mechanism or via a dissociative mechanism with a genuine five-coordinate intermediate. In the twist mechanism, rearrangement occurs via rotation about a pseudo-3-fold axis of the idealized coordination octahedron. A pseudorotation mechanism has been suggested to be operative in $Re^{V}O$(dithiolate)(CH_3)(L) complexes[34] and *cis*/*trans*-$Mo^{V}O(NNO)Cl_2$ as well as $Mo^{VI}O_2(NNO)Cl$ complexes (NNO = heteroscorpionato ligand).[35] The dissociative mechanism proceeds via ligand loss, subsequent Berry or turnstile pseudorotation of the five-coordinate intermediate, and recoordination at a stereochemically different site. A dissociative mechanism has been invoked in *cis*/*trans*-$Re^{V}O(CH_3)_2Cl$(bpy) via a monodentate 2,2′-bipyridine (bpy) ligand.[36] Hemilability of a bpy chelate has also been suggested for $FeEt_2(bpy)_2$.[37] Potentially labile Mo−ligand bonds in **1** are certainly the Mo−C or Mo−N^{i} bonds, while the Mo═O multiple bond and the Mo−N^{p} bonds are considered to be much stronger. The possibility of Mo−C cleavage is supported by the mass spectrum of **1** showing M^+ and $[M - CN^tBu]^+$ peaks, albeit for the cation. Naturally, intermediate partial dissociation of a chelate N^{i} donor would be invisible to mass spectrometric analysis.

dx.doi.org/10.1021/ic4025102 | *Inorg. Chem.* 2014, 53, 1039−1047

Table 1. Experimental and DFT-Calculated[a] Relevant Metrical (Å and deg), Vibrational (cm^{-1}), and Energy Data (kJ mol^{-1}) of 1−4

	X-ray **1** (x = a; y = b)	DFT **1** (x = a; y = b)	DFT **2** (x = c; y = d)	DFT **3** (x = e; y = f)	DFT **4** (x = g; y = h)
Mo1−O1	1.6850(15)	1.701 (1.708)	1.703 (1.709)	1.691 (1.699)	1.690 (1.698)
Mo1−C1	2.1093(22)	2.108 (2.120)	2.126 (2.136)	2.098 (2.110)	2.114 (2.127)
Mo1−$N^{x,i}$	2.2135(17)	2.285 (2.285)	2.229 (2.231)	2.493 (2.475)	2.507 (2.493)
Mo1−$N^{x,p}$	2.2422(17)	2.273 (2.268)	2.312 (2.306)	2.186 (2.193)	2.165 (2.170)
Mo1−$N^{y,i}$	2.1980(17)	2.252 (2.254)	2.202 (2.203)	2.236 (2.236)	2.229 (2.227)
Mo1−$N^{y,p}$	2.1074(18)	2.119 (2.116)	2.142 (2.141)	2.136 (2.131)	2.134 (2.131)
C1−N1	1.1552(27)	1.177 (1.174)	1.177 (1.175)	1.178 (1.175)	1.178 (1.175)
Mo1−C1−N1	176.25(19)	179.3 (179.8)	177.6 (178.4)	179.7 (179.2)	176.6 (176.1)
C1−Mo1−O1	93.76(8)	94.1 (94.2)	90.8 (90.7)	95.7 (95.6)	92.5 (92.6)
$\tilde{\nu}$(Mo═O)	937	947 (927)[b]	946 (928)[b]	965 (942)[b]	967 (945)[b]
$\tilde{\nu}$(C≡N)	2129	2117 (2129)[b]	2124 (2130)[b]	2113 (2122)[b]	2113 (2121)[b]
$\Delta G°$(298 K)		0.0 (0.0)	1.1 (2.5)	5.6 (5.8)	7.4 (9.5)

[a]From model complexes with the *tert*-butyl group of the chelate ligands replaced by hydrogen atoms; gas-phase calculations; PCM(THF) data in parentheses. [b]Calculated harmonic frequencies are scaled by 0.9614.[33]

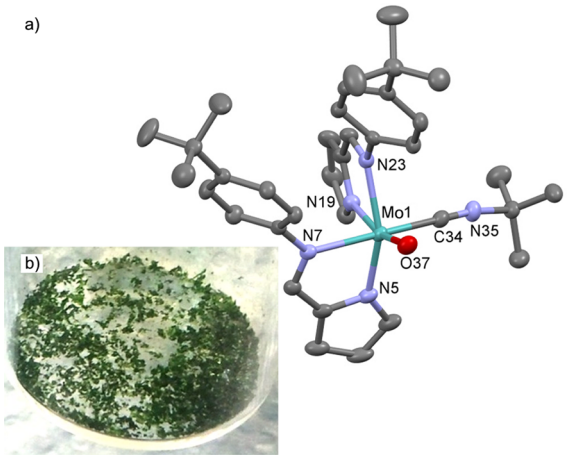

Figure 3. (a) Molecular structure of **1** in the crystal (hydrogen atoms omitted for clarity; thermal ellipsoids with 50% probability) and (b) photograph of crystals of **1**.

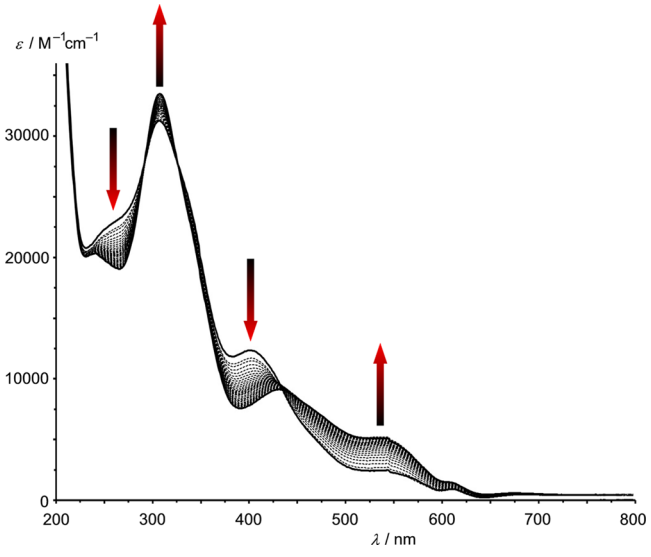

Figure 4. UV/vis spectra of $Mo^{IV}O(N^{p}{\cap}N^{i})_2(CN^{t}Bu)$ in THF after dissolution of crystals of **1** at −30 °C and warming to +25 °C.

Isocyanide dissociation has been calculated by DFT methods from **1** and **2** to give the five-coordinate cis and trans isomers **5**,

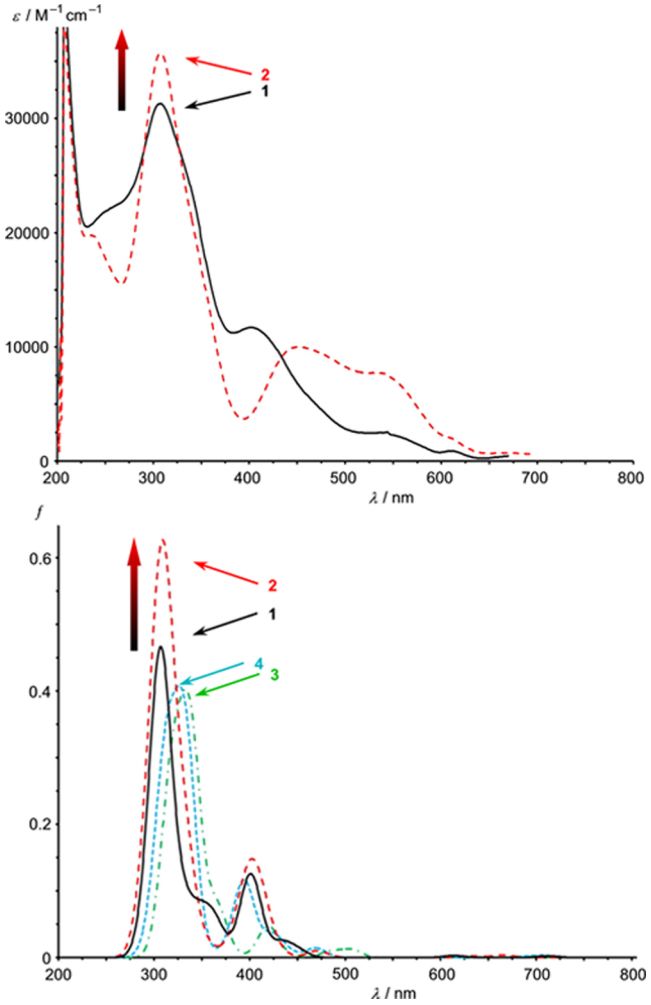

Figure 5. UV/vis spectra of **1** in THF (black —) and of **2** (obtained from the difference spectrum "**1**/**2** mixture *minus* **1**") in THF (red - - -) [top] and those from TD-DFT calculations of **1** (black —), **2** (red - - -), **3** (green ···), and **4** (blue ···) and Lorentzian band shapes with fwhm 25 cm^{-1} [bottom].

respectively (Chart 2). The free energies of activation are calculated as 83 and 63 kJ mol^{-1} for TS(Λ-**1**→*cis*-**5**) and TS(Λ-**2**→*trans*-**5**), respectively (Figure 6), which are reasonable values for $CN^{t}Bu$ dissociation from Mo^{IV}. The necessary five-

dx.doi.org/10.1021/ic4025102 | *Inorg. Chem.* 2014, 53, 1039−1047

Chart 2. Five-Coordinate Complexes *cis*- and *trans*-5

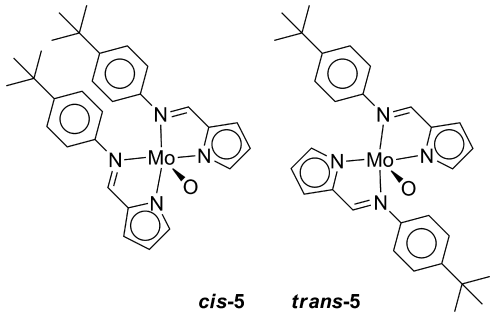

coordinate turnstile transition states for isomerization from *cis*-**5** to *trans*-**5** are TS1(*cis*-**5**→*trans*-**5**) and TS2(*cis*-**5**→*trans*-**5**) with N^p or N^i in pseudoapical positions (Figure 6). These transition states are calculated with barriers of 149/148 kJ mol^{-1}, which seem to be quite high. The calculations suggest that the Mo−N^i bond of one chelate is elongated during pseudorotation. In summary, the turnstile rotation requires much more energy than CN^{t}Bu dissociation and becomes the rate-determining step (rds) in this mechanism. For completeness, the barriers for CN^{t}Bu dissociation from **3** to *trans*-**5** and **4** to *cis*-**5** have also been calculated as 90 and 76 kJ mol^{-1} (see the SI).

Pseudorotation of the trigonal face spanned by O, C, and one N^i against the opposite trigonal plane (trigonal-twist mechanism) gives isomer Δ-**2** from Λ-**1** at much lower energy cost (65 kJ mol^{-1}; Figure 7). Inspection of the pseudo-trigonal-prismatic transition-state structure TS(Λ-**1**→Δ-**2**) reveals that during the twist one Mo−N^i bond is completely disrupted. Hence, the mechanism of isomerization is best described by a dissociative pseudorotation involving a N^i donor dissociation of one chelate ligand. This interpretation is in accordance with the

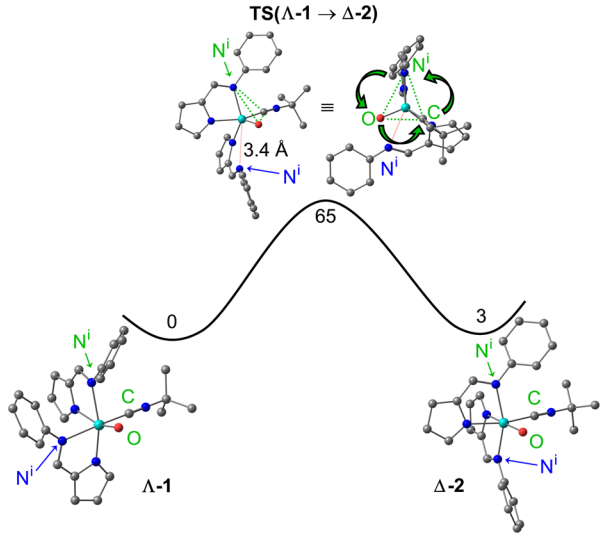

Figure 7. Calculated energy profile [ΔG°(298 K)/kJ mol^{-1}] of the isomerization of Λ-**1** to Δ-**2** via a dissociative twist (B3LYP/LANL2DZ/PCM THF; hydrogen atoms omitted for clarity).

mechanism proposed for the cis/trans isomerization of $ReO(CH_3)_2Cl(bpy)$ on the basis of its small positive activation entropy and rate independence of added bpy.[36] Because in both calculated scenarios the rds, namely, either TS(*cis*-**5**→*trans*-**5**) or TS(Λ-**1**→Δ-**2**), is unimolecular, the equilibration rate should not be diminished by the presence of excess CN^{t}Bu in either case. Indeed, in the presence of 2, 10, or 100 equiv of CN^{t}Bu, the reaction is not slowed. The reaction proceeds even faster according to ^{1}H NMR measurements. 50% conversion at room temperature is achieved at 895, 350, 155 and <100 s for 0, 2, 10, and 100 equiv of CN^{t}Bu added. This points to the possibility of an additional associative (or interchange I_a)

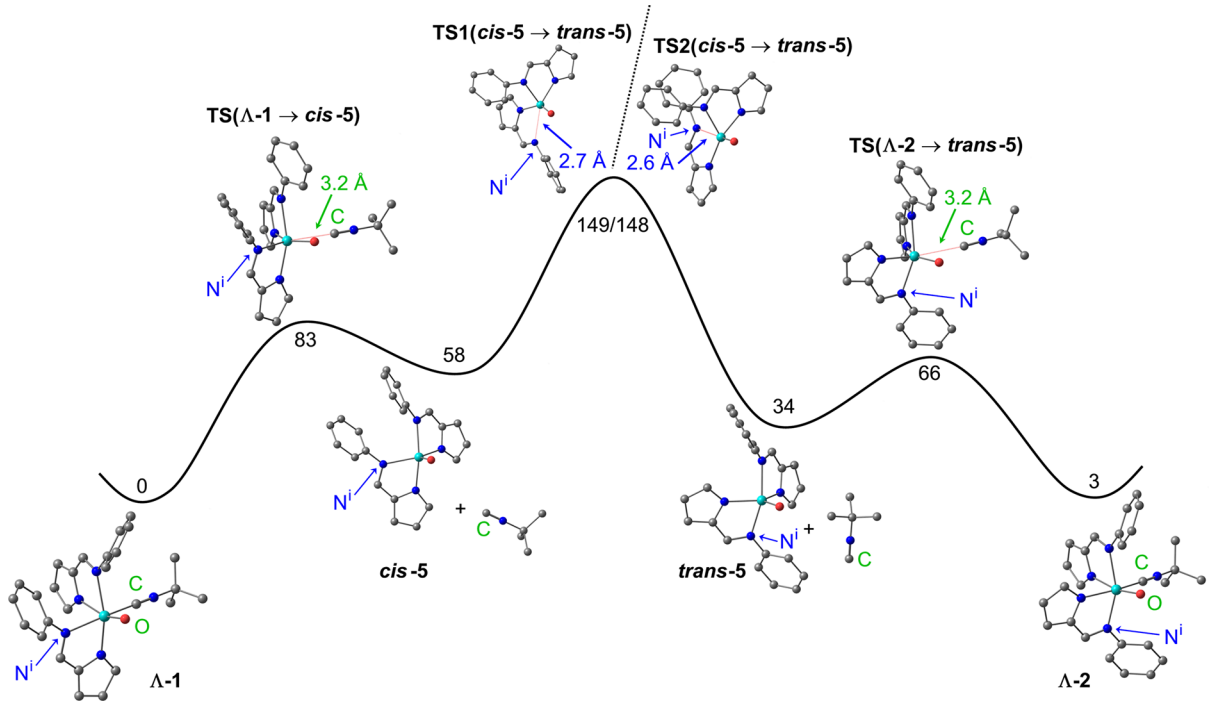

Figure 6. Calculated energy profile [ΔG°(298 K)/kJ mol^{-1}] of the isomerization of Λ-**1** to -**2** via *cis*- and *trans*-**5** intermediates (B3LYP/LANL2DZ/PCM THF; hydrogen atoms omitted for clarity).

dx.doi.org/10.1021/ic4025102 | *Inorg. Chem.* 2014, 53, 1039−1047

pathway in the presence of excess CN^{t}Bu. In the absence of excess CN^{t}Bu, this pathway seems to play only a minor role.

With the condition that the rds in the isomerization equilibrium **1** to **2** (without added CN^{t}Bu) is first order in **1**, we studied the process by ^{1}H NMR spectroscopy at different temperatures and analyzed the reaction progress according to a first-order process. From time-dependent ^{1}H NMR measurements performed between 288 and 318 K, time traces of the evolution of **1** to **2** were obtained from integration of H^7 proton resonances at δ 8.41 (H^{7d}) of isomer **2** or isocyanide proton resonances of **2** at δ 1.01. Other isomers **3** and **4** were neglected. No accumulation of free isocyanide is observed during equilibration. The experimental data have been fitted to the rate law of a reversible first-order reaction $d[\mathbf{2}]/dt = k_f[\mathbf{1}] - k_b[\mathbf{2}]$

$$[\mathbf{2}] = \{[\mathbf{1}]_{t=0}/(k_f + k_b)\}\{k_f - k_f \exp[-(k_f + k_b)t]\}$$

and rate constants k_f at different temperatures have been extracted. Eyring–Polanyi plots give $\Delta H^{\ddagger}_f$ = 91 and 95 kJ mol^{-1} in THF-d_8 and toluene-d_8, respectively (Figure S4 in the SI). Because of the large errors associated with determination of the activation entropies using this small temperature range, we refrain from discussing $\Delta S^{\ddagger}$ values. However, the similarity of the activation enthalpies in THF and toluene suggests that the solvent plays only a minor role in the rds, and an associative rds involving THF is safely excluded.[38] However, the experimental data do not distinguish between the two rather dissociative first-order mechanisms (Figures 6 and 7).

Hence, the molybdenum(IV) oxido isocyanide complexes **1** and **2** are stereochemically flexible but appear stable toward (irreversible) ligand loss. **1** and **2** are even stable in the presence of hydroxide (phosphazene base P$_1^t$Bu and H$_2$O), and attack of hydroxide at either molybdenum or the isocyanide ligand is not detected by NMR. One-electron-oxidation reactions of these stable molybdenum(IV) complexes **1** and **2** to molybdenum(V) and their much more complex reactivity will be reported in a separate contribution.

CONCLUSION

In this study, we aimed at obtaining a simple (copper-deficient) CODH analogue system with a carbon-based substrate (CN^{t}Bu) bound to molybdenum in the biologically relevant oxidation state IV+. OAT from $MoO_2(N^p{\cap}N^i)_2$ to CN^{t}Bu was not observed; however, PMe_3 ligand displacement from $MoO(N^p{\cap}N^i)_2(PMe_3)$ was feasible to give stereoisomerically pure molybdenum(IV) oxido isocyanide complex **1** after recrystallization. Its solid-state structure has been determined by X-ray diffraction. The CN^{t}Bu ligand is coordinated in an end-on fashion to Mo^{IV} rather than in a η^2-OCN^{t}Bu fashion, as suggested in the Hofmann intermediate (Scheme 1). However, the stereoisomer **1** equilibrates with the Δ,Λ-OC-6-2-4 stereoisomer **2** in solution at ambient temperature. The configurations of both diastereomers have been elucidated by NMR, IR, and UV/vis spectroscopy in combination with DFT/PCM and TD-DFT calculations. Mechanistically, the isomerization **1** → **2** is suggested to proceed via a dissociative trigonal twist with dissociation of the imine nitrogen donor N^i of one chelate ligand (hemilabile ligand) rather than dissociation of the monodentate isocyanide ligand. The isomerization barrier has been determined as 91 and 95 kJ mol^{-1} in THF and toluene, respectively. The stability of the Mo^{IV}–C bond in **1** and **2** paves the way for future investigations with respect to higher oxidation states of molybdenum and with relevance for biomimetic oxygenation reactions of carbon-based substrates.

ASSOCIATED CONTENT

Supporting Information

NMR spectra of **1** and the **1** + **2** mixture, IR spectra of **1** and the **1** + **2** mixture, Eyring–Polanyi plots, and Cartesian coordinates and energies of all optimized structures. This material is available free of charge via the Internet at http://pubs.acs.org.

AUTHOR INFORMATION

Corresponding Author

*E-mail: katja.heinze@uni-mainz.de. Fax: +49-6131-39-27277.

Author Contributions

The manuscript was written through contributions of all authors. All authors have given approval to the final version of the manuscript.

Notes

The authors declare no competing financial interest.

ACKNOWLEDGMENTS

We are grateful to Dr. Mihail Mondeshki for excellent NMR support and to Regine Jung-Pothmann and Dr. Dieter Schollmeyer for X-ray data collection.

REFERENCES

(1) Holm, R. H. *Chem. Rev.* **1987**, *87*, 1401–1449.
(2) (a) Dobbek, H.; Gremer, L.; Meyer, O.; Huber, R. In *Handbook of Metalloproteins*; Messerschmidt, A., Huber, R., Wieghardt, K., Poulos, T., Eds.; Wiley: Chichester, U.K., 2001; Vol. 2, pp 1136–1147. (b) Enemark, J. H.; Cooney, J. J. A.; Wang, J.-J.; Holm, R. H. *Chem. Rev.* **2004**, *104*, 1175–1200. (c) Schulzke, C. *Eur. J. Inorg. Chem.* **2011**, 1189–1199. (d) Sugimoto, H.; Tsukube, H. *Chem. Soc. Rev.* **2008**, *37*, 2609–2619.
(3) Dobbek, H.; Gremer, L.; Kiefersauer, R.; Huber, R.; Meyer, O. *Proc. Natl. Acad. Sci. U.S.A.* **2002**, *99*, 15971–15976.
(4) Gourlay, C.; Nielsen, D. J.; White, J. M.; Knottenbelt, S. Z.; Kirk, M. L.; Young, C. G. *J. Am. Chem. Soc.* **2006**, *128*, 2164–2165.
(5) Hofmann, M.; Kassube, J. K.; Graf, T. *J. Biol. Inorg. Chem.* **2005**, *10*, 490–495.
(6) Siegbahn, P. E. M.; Shestakov, A. F. *J. Comput. Chem.* **2005**, *26*, 888–898.
(7) Pilato, R. S.; Geoffroy, G. L.; Rheingold, A. L. *J. Chem. Soc., Chem. Commun.* **1989**, 1287–1288.
(8) Yonke, B. L.; Reeds, J. P.; Zavalij, P. Y.; Sita, L. R. *Angew. Chem.* **2011**, *123*, 12550–12554; *Angew. Chem., Int. Ed.* **2011**, *50*, 12342–12346.
(9) Heinze, K.; Fischer, A. *Eur. J. Inorg. Chem.* **2007**, 1020–1026.
(10) Heinze, K.; Marano, G.; Fischer, A. *J. Inorg. Biochem.* **2008**, *102*, 1199–1211.
(11) Heinze, K.; Fischer, A. *Eur. J. Inorg. Chem.* **2010**, 1939–1947.
(12) Hüttinger, K.; Förster, C.; Bund, T.; Hinderberger, D.; Heinze, K. *Inorg. Chem.* **2012**, *51*, 4180–4192.
(13) Novotny, M.; Lippard, S. J. *Inorg. Chem.* **1974**, *13*, 828–831.
(14) Re, R. E. D.; Hopkins, M. D. *Inorg. Chem.* **2002**, *41*, 6973–6985.
(15) Tran, B. L.; Carrano, C. J. *Inorg. Chem.* **2007**, *46*, 5429–5438.
(16) Söncksen, L.; Römer, R.; Näther, C.; Peters, G.; Tuczek, F. *Inorg. Chim. Acta* **2011**, *374*, 472–479.
(17) Greco, G. E.; O'Donoghue, M. B.; Seidel, S. W.; Davis, W. M.; Schrock, R. R. *Organometallics* **2000**, *19*, 1132–1149.
(18) Carmona, E.; Galindo, A.; Guille-Photin, C.; Sanchez, L. *Polyhedron* **1988**, *7*, 1767–1771.
(19) Montilla, F.; Galindo, A.; Carmona, E.; Gutiérrez-Puebla, E.; Monge, A. *J. Chem. Soc., Dalton Trans.* **1998**, 1299–1305.

(20) Bryan, J. C.; Mayer, J. M. *J. Am. Chem. Soc.* **1990**, *112*, 2298−2308.
(21) Hall, K. A.; Mayer, J. M. *J. Am. Chem. Soc.* **1992**, *114*, 10402−10411.
(22) *SMART Data Collection and SAINT-Plus Data Processing Software for the SMART System (various versions)*; Bruker Analytical X-ray Instruments, Inc.: Madison, WI, 2000.
(23) *SADABS*; Bruker AXS Inc.: Madison, WI, 2001.
(24) Sheldrick, G. M. *SHELXTL*, version 5.1; Bruker AXS: Madison, WI, 1998.
(25) Sheldrick, G. M. *SHELXL-97*; University of Göttingen: Göttingen, Germany, 1997.
(26) Frisch, M. J.; Trucks, G. W.; Schlegel, H. B.; Scuseria, G. E.; Robb, M. A.; Cheeseman, J. R.; Scalmani, G.; Barone, V.; Mennucci, B.; Petersson, G. A.; Nakatsuji, H.; Caricato, M.; Li, X.; Hratchian, H. P.; Izmaylov, A. F.; Bloino, J.; Zheng, G.; Sonnenberg, J. L.; Hada, M.; Ehara, M.; Toyota, K.; Fukuda, R.; Hasegawa, J.; Ishida, M.; Nakajima, T.; Honda, Y.; Kitao, O.; Nakai, H.; Vreven, T.; Montgomery, J. A., Jr.; Peralta, J. E.; Ogliaro, F.; Bearpark, M.; Heyd, J. J.; Brothers, E.; Kudin, K. N.; Staroverov, V. N.; Kobayashi, R.; Normand, J.; Raghavachari, K.; Rendell, A.; Burant, J. C.; Iyengar, S. S.; Tomasi, J.; Cossi, M.; Rega, N.; Millam, J. M.; Klene, M.; Knox, J. E.; Cross, J. B.; Bakken, V.; Adamo, C.; Jaramillo, J.; Gomperts, R.; Stratmann, R. E.; Yazyev, O.; Austin, A. J.; Cammi, R.; Pomelli, C.; Ochterski, J. W.; Martin, R. L.; Morokuma, K.; Zakrzewski, V. G.; Voth, G. A.; Salvador, P.; Dannenberg, J. J.; Dapprich, S. Daniels, A. D.; Farkas, O.; Foresman, J. B.; Ortiz, J. V.; Cioslowski, J.; Fox, D. J. *Gaussian 09*, revision A.02; Gaussian, Inc.: Wallingford, CT, 2009.
(27) Huzinaga, S.; Andzelm, J.; Klobukowski, M.; Radzio-Andzelm, E.; Sakai, Y.; Tatewaki, H. *Gaussian Basis Sets for Molecular Orbital Calculations*; Elsevier: Amsterdam, The Netherlands, 1984.
(28) The stereochemistry of the complexes under study will be described by the configuration index according to the Cahn−Ingold−Prelog system in an octahedral complex OC-6-*x*-*y* with the priority sequence used as follows: O > $N^{pyrrolato}$ > N^{imine} > $C^{isocyanide}$. The first index *x* refers to the ligand priority of the ligand trans to the ligand of the highest priority (axial ligands) and the second index *y* refers to the ligand priority trans to that ligand of the equatorial plane, which has the highest priority of these four equatorial ligands. Thus, molybdenum(IV) complex **1** possesses OC-6-2-3 stereochemistry, as depicted in Chart 1.
(29) Cahn, R. S.; Ingold, C. K.; Prelog, V. *Angew. Chem., Int. Ed. Engl.* **1966**, *5*, 385−415.
(30) Prelog, V.; Helmchen, G. *Angew. Chem., Int. Ed. Engl.* **1982**, *21*, 567−583.
(31) Block, B. P.; Powell, W. H.; Fernelius, W. C. *Inorganic chemical nomenclature:principles and practice*; ACS Professional Reference Book; American Chemical Society: Washington, DC, 1990.
(32) von Zelewsky, A. *Stereochemistry of Coordination Compounds*; John Wiley & Sons Ltd.: New York, 1996.
(33) Koch, W.; Holthausen, M. C. *A Chemist's Guide to Density Functional Theory*; Wiley-VCH: Weinheim, Germany, 2001; p 134.
(34) Lahiti, D. W.; Espenson, J. H. *J. Am. Chem. Soc.* **2001**, *123*, 6014−6024.
(35) (a) Kail, B.; Nemykin, V. N.; Davie, S. R.; Carrano, C. J.; Hammes, B.; Basu, P. *Inorg. Chem.* **2002**, *41*, 1281−1291. (b) Hoffman, J. T.; Einwaechter, S.; Chohan, B. S.; Basu, P.; Carrano, C. J. *Inorg. Chem.* **2004**, *43*, 7573−7575. (c) Hoffman, J. T.; Tran, B. L.; Carrano, C. J. *Dalton Trans.* **2006**, 3822−3830. (d) Kail, B. W.; Basu, P. *Dalton Trans.* **2006**, 1419−1423.
(36) Jung, J.-H.; Albright, T. A.; Hoffman, D. M.; Lee, T. R. *J. Chem. Soc., Dalton Trans.* **1999**, 4487−4494.
(37) Yamamoto, T.; Yamamoto, A.; Ikeda, S. *Bull. Chem. Soc. Jpn.* **1972**, *45*, 1104−1110.
(38) Helm, L.; Merbach, A. E. *Chem. Rev.* **2005**, *105*, 1923−1959.